

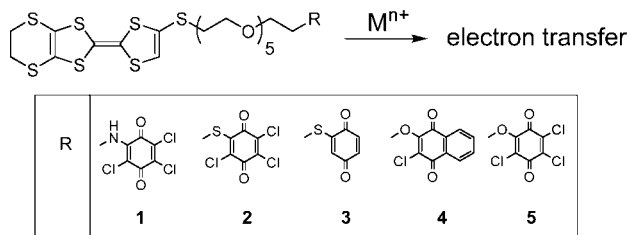
New Substituted Tetrathiafulvalene–Quinone Dyads: The Influences of Electron Accepting Abilities of Quinone Units on the Metal Ion-Promoted Electron-Transfer Processes

Hui Wu,^{†,‡} Deqing Zhang,^{*†} Guanxin Zhang,[†] and Daoben Zhu^{*†}

Beijing National Laboratory for Molecular Sciences, Organic Solids Laboratory, Institute of Chemistry, Chinese Academy of Sciences, Beijing 100080, and Graduate School of Chinese Academy of Sciences, Beijing 100080, China

dqzhang@iccas.ac.cn

Received March 14, 2008



The metal ion-promoted electron transfer occurs to all new dyads **1**, **2**, **3**, and **4**, even one of them, dyad **4**, which has a rather weak electron acceptor unit. The results also indicate that the metal ion-promoted electron transfer within the dyads is influenced by the electron accepting abilities of quinone units; dyad **2** with the strongest electron acceptor among the four dyads shows the strongest absorption and ESR signals attributed to TTF^{•+} in the presence of metal ions.

Tetrathiafulvalene (TTF) and its derivatives are strong electron donors (D). Various electron acceptors (A) have been connected to TTF to afford electron donor–acceptor (D–A) dyads or triads for investigations of charge-transfer interactions and building molecular level devices, such as molecular rectifiers¹ and molecular switches.² For instance, a new redox fluorescence switch and some chemical sensors based on the TTF–anthracene dyad were reported;³ the excited property of anthracene within the TTF–anthracene dyad can be tuned by assembly on the surfaces of gold nanoparticles.⁴ D–A dyads with TTF and perylene diimide analogues were synthesized and their fluorescence intensities varied with the oxidation states of TTF units.⁵

We have recently reported a TTF–trichloroquinone dyad linked by an oligoethylene glycol chain.⁶ For this D–A dyad, the metal ion-promoted electron transfer was observed and moreover the electron transfer process can be reversibly tuned

by alternating UV and visible light irradiations in the presence of spiropyran. It would be interesting to see whether the metal ion-promoted electron transfer can occur to TTF–A dyads with electron acceptor units showing different redox potentials, and examine the influence of the electron-accepting abilities on the metal ion-promoted electron transfer processes. For these purposes, substituted TTF–quinone dyads **1**, **2**, **3**, **4**, and **5**⁶ (Scheme 1), whose quinone units exhibit different electron-accepting behaviors, were synthesized and their electron transfer properties were investigated in the presence of metal ions. The TTF and quinone units are linked by the oligoethylene glycol chain.^{7,8} Substituted quinones **12**, **13**, **14**, and **15** (Scheme 1) were synthesized and dyad **5** was also included for comparison.

The synthesis of substituted TTF–quinone dyads **1**, **2**, **3**, and **4** started from compound **6**. After reaction with *p*-toluenesulfonyl chloride in the presence of triethylamine, compound **6** was transformed into compound **7** in 86% yield, which was further reacted with potassium thioacetate to make compound **8**. Reduction of compound **8** with LiAlH₄ yielded compound **9**,

(1) See for examples: (a) Nielsen, M. B.; Hansen, J. G.; Becher, J. *Eur. J. Org. Chem.* **1999**, 2807–2815. (b) Hansen, J. G.; Bang, K. S.; Thorup, N.; Becher, J. *Eur. J. Org. Chem.* **2000**, 2135–2144. (c) Simonsen, K. B.; Zong, K.; Rogers, R. D.; Cava, M. P.; Becher, J. *J. Org. Chem.* **1997**, *62*, 679–686. (d) Simonsen, K. B.; Thorup, N.; Cava, M. P.; Becher, J. *Chem. Commun.* **1998**, 901–902. (e) Perepichka, D. F.; Bryce, M. R.; McInnes, E. J. L.; Zhao, J. *Org. Lett.* **2001**, *3*, 1431–1434. (f) Metzger, R. M. *Acc. Chem. Res.* **1999**, *32*, 950–957. (g) Metzger, R. M.; Chen, B.; Höpfner, U.; Lakshmikantham, M. V.; Vuillaume, D.; Kawai, T.; Wu, X.; Tachibana, H.; Hughes, T. V.; Sakurai, H.; Baldwin, J. W.; Hosch, C.; Cava, M. P.; Brehmer, L.; Ashwell, G. J. *J. Am. Chem. Soc.* **1997**, *119*, 10455–10466. (h) Diaz, M. C.; Illescas, B. M.; Martín, N.; Viruela, R.; Viruela, P. M.; Ortí, E.; Brede, O.; Zilbermann, I.; Guldi, D. M. *Chem. Eur. J.* **2004**, *10*, 2067–2077. (i) Giacalone, F.; Segura, J. L.; Martín, N.; Guldi, D. M. *J. Am. Chem. Soc.* **2004**, *126*, 5340–5341. (j) Perepichka, D. F.; Bryce, M. R.; Batsanov, A. S.; McInnes, E. J. L.; Zhao, J. P.; Farley, R. D. *Chem. Eur. J.* **2002**, *8*, 4656–4669. (k) Ho, G.; Heath, J. R.; Kondratenko, M.; Perepichka, D. F.; Arseneault, K.; Pézolet, M.; Bryce, M. R. *Chem. Eur. J.* **2005**, *11*, 2914–2922.

(2) (a) Bryce, M. R. *Adv. Mater.* **1999**, *11*, 11–23. (b) Bryce, M. R. *J. Mater. Chem.* **2000**, *10*, 589–598. (c) Segura, J. L.; Martín, N. *Angew. Chem., Int. Ed.* **2001**, *40*, 1372–1409, and further references cited therein. (d) Farren, C.; Christensen, C. A.; FitzGerald, S.; Bryce, M. R.; Beeby, A. *J. Org. Chem.* **2002**, *67*, 9130–9139. (e) Nielsen, M. B.; Nielsen, S. B.; Becher, J. *Chem. Commun.* **1998**, 475–476. (f) Li, H.; Jeppesen, J. O.; Levillain, E.; Becher, J. *Chem. Commun.* **2003**, 846–847. (g) Liu, Y.; Flood, A. H.; Stoddart, J. F. *J. Am. Chem. Soc.* **2004**, *126*, 9150–9151. (h) Xiao, X.; Xu, W.; Zhang, D.; Xu, H.; Lu, H.; Zhu, D. *J. Mater. Chem.* **2005**, *15*, 2557–2561. (i) Zhou, Y.; Zhang, D.; Zhu, L.; Shuai, Z.; Zhu, D. *J. Org. Chem.* **2006**, *71*, 2123–2130.

(3) (a) Zhang, G.; Zhang, D.; Guo, X.; Zhu, D. *Org. Lett.* **2004**, *6*, 1209–1212. (b) Li, X.; Zhang, G.; Ma, H.; Zhang, D.; Li, J.; Zhu, D. *J. Am. Chem. Soc.* **2004**, *126*, 11543–11548. (c) Zhang, G.; Li, X.; Ma, H.; Zhang, D.; Li, J.; Zhu, D. *Chem. Commun.* **2004**, 2072–2073. (d) Feng, M.; Guo, X.; Lin, X.; He, X.; Ji, W.; Du, S.; Zhang, D.; Zhu, D.; Gao, H. *J. Am. Chem. Soc.* **2005**, *127*, 15338–15339. (e) Lu, H.; Xu, W.; Zhang, D.; Chen, C.; Zhu, D. *Org. Lett.* **2005**, *7*, 4629–4632. (f) Zhang, G.; Zhang, D.; Zhou, Y.; Zhu, D. *J. Org. Chem.* **2006**, *71*, 3970–3972. (g) Wen, G.; Zhang, D.; Huang, Y.; Zhao, R.; Zhu, L.; Shuai, Z.; Zhu, D. *J. Org. Chem.* **2007**, *72*, 6247–6250.

(4) Zhang, G.; Zhang, D.; Zhao, X.; Ai, X.; Zhang, J.; Zhu, D. *Chem. Eur. J.* **2006**, *12*, 1067–1073.

(5) (a) Guo, X.; Zhang, D.; Zhang, H.; Fan, Q.; Xu, W.; Ai, X.; Fan, L.; Zhu, D. *Tetrahedron* **2003**, *59*, 4843–4850. (b) Leroy-Lhez, S.; Baffreau, J.; Perrin, L.; Levillain, E.; Allain, M.; Blesa, M.-J.; Hudhomme, P. *J. Org. Chem.* **2005**, *70*, 6313–6320. (c) Zheng, X.; Zhang, D.; Zhu, D. *Tetrahedron Lett.* **2006**, *47*, 9083–9087. (d) Guo, X.; Gan, Z.; Luo, H.; Araki, Y.; Zhang, D.; Zhu, D.; Ito, O. *J. Phys. Chem. A* **2003**, *107*, 9747–9753.

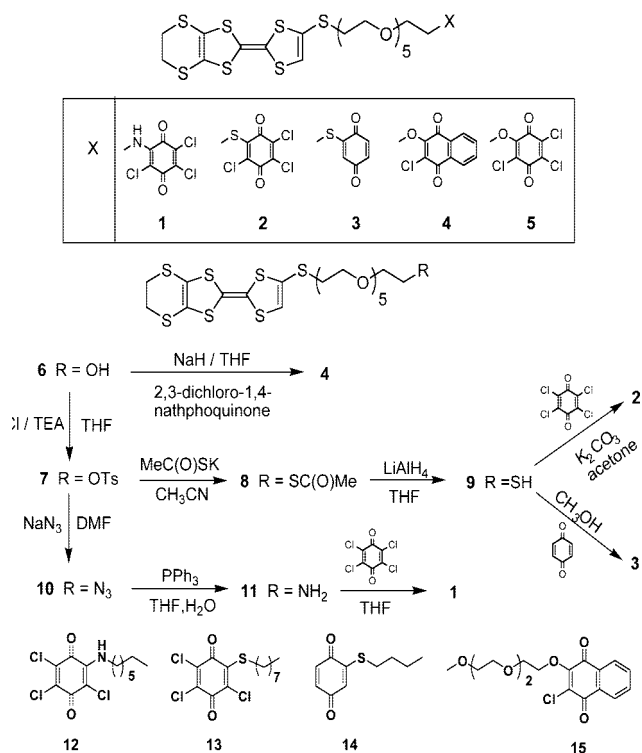
(6) Wu, H.; Zhang, D.; Su, L.; Ohkubo, K.; Zhang, C.; Yin, S.; Mao, L.; Shuai, Z.; Fukuzumi, S.; Zhu, D. *J. Am. Chem. Soc.* **2007**, *129*, 6839–6846.

(7) For other examples of TTF–quinone systems, see: (a) Dumur, F.; Gautier, N.; Gallego-Planas, N.; Sahin, Y.; Levillain, E.; Mercier, N.; Hudhomme, P.; Masino, M.; Giraldo, A.; Lloveras, V.; Vidal-Gancedo, J.; Veciana, J.; Rovira, C. *J. Org. Chem.* **2004**, *69*, 2164–2177, and further references therein. (b) Scheib, S.; Cava, M. P.; Baldwin, J. W.; Metzger, R. M. *J. Org. Chem.* **1998**, *63*, 1198–1204.

[†] Chinese Academy of Sciences.

[‡] Graduate School of Chinese Academy of Sciences.

SCHEME 1. The Chemical Structures of Dyads **1**, **2**, **3**, **4**, and **5** and the Reference Compounds **12**–**15** as Well as the Synthetic Scheme



which reacted with tetrachloro-1,4-benzoquinone and 1,4-benzoquinone directly to afford dyad **2** and dyad **3** in 41% and 52% yields, respectively. For the synthesis of dyad **1**, compound **7** was converted to compound **10** after reaction with NaN₃. Compound **11** was obtained by reaction of compound **10** with PPh₃, and further reaction of compound **11** with tetrachloro-1,4-benzoquinone yielded dyad **1** in 31% yield. Dyad **4** was obtained by direct reaction of compound **6** with 2,3-dichloro-1,4-naphthoquinone in the presence of NaH. The detailed synthetic procedures and characterizations are provided in the Supporting Information. Reference quinone compounds **12**, **13**, **14**, and **15** were also synthesized according to reported procedures (see the Supporting Information).

The redox potentials were measured and the results are listed in Table 1. The oxidation potentials of dyads **1**, **2**, **3**, and **4** are almost the same as those of dyad **5**, and their reduction potentials are almost the same as those of reference quinone compounds **12**, **13**, **14**, and **15**.⁹ These cyclic voltammetric data show that there is no detectable interaction between TTF and quinone units within these D–A dyads. The electron-accepting abilities of the quinone units within dyads **1**, **2**, **3**, **4**, and **5**⁶ decreased in the following order: **2** > **5** > **1** > **3** > **4**.

The absorption spectra of dyads **1**, **2**, **3**, and **4** were measured in the presence of Pb²⁺, Zn²⁺, and Sc³⁺. In all cases, new

TABLE 1. The Redox Potentials (vs. Ag/AgCl) of Dyads **1**, **2**, **3**, **4**, and **5**, Oxidation Potentials of **6**, and Reduction Potentials of Reference Quinone Compounds **12**, **13**, **14**, and **15**^a

compd	$E^{1/2}_{ox1}$, V	$E^{1/2}_{ox2}$, V	$E^{1/2}_{red1}$, V
1	0.50	0.84	−0.32
2	0.49	0.84	−0.06
3	0.50	0.83	−0.47
4	0.50	0.83	−0.60
5	0.50	0.84	−0.09
6	0.50	0.83	
12			−0.32
13			−0.06
14			−0.48
15			−0.59

^a Cyclic voltammetric measurements were performed with platinum wires as working and counter electrodes, and Ag/AgCl electrode (saturated KCl) as the reference electrode, respectively. The scan rate was 100 mV S^{−1}. *n*-Bu₄NPF₆ (0.1 M) was used as the supporting electrolyte. The concentration of each compound was 1.0 × 10^{−3} in a mixture of CH₂Cl₂ and CH₃CN (1:1, v/v).

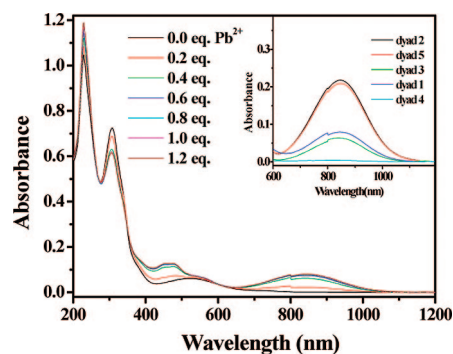


FIGURE 1. Absorption spectra of dyad **1** recorded in a mixture of CH₂Cl₂ and CH₃CN (1:1, v/v; 5.0 × 10^{−5} M) in the presence of increasing amounts of Pb²⁺ [Pb(ClO₄)₂]; the inset shows the 600–1200 nm part of the absorption spectra of dyads **1**, **2**, **3**, **4**, and **5** in the presence of 1.0 equiv of Pb²⁺ [Pb(ClO₄)₂].

absorptions around 450 and 845 nm (see Figures S1–S11 of the Supporting Information) were observed. For instance, Figure 1 shows the absorption spectrum of dyad **1** and those in the presence of different amounts of Pb²⁺. Before the addition of Pb²⁺, dyad **1** exhibits no absorption above 600 nm. However, new absorptions around 450 and 845 nm appear in the presence of Pb²⁺; moreover, the absorption intensities at 450 and 845 nm increased with increasing amounts of Pb²⁺ as shown in Figure 1. According to previous studies,^{21,6,10} the absorption bands around 450 and 845 nm could be ascribed to the radical cation of TTF (TTF^{•+}) units of D–A dyads. This assumption was supported by the control experiments with compound **6**; both chemical oxidation of **6** by addition Fe³⁺ and electrochemical oxidations of **6** by applying an oxidation potential at +0.65 V (vs Ag/AgCl) led to new absorption bands at 450 and 845 nm (see Figures S13 and S14 of the Supporting Information). The possibility that these new absorptions of dyads **1**, **2**, **3**, and **4** in the presence of metal ions are due to the charge transfer from the TTF to quinone units can be ruled out on the

(8) For recent examples of metal complexation of polyether–TTFs, see: (a) Trippé, G.; Le Derf, F.; Lyskawa, J.; Mazari, M.; Roncali, J.; Gorgues, A.; Levillain, E.; Sallé, M. *Chem. Eur. J.* **2004**, *10*, 6497–6509. (b) Lyskawa, J.; Le Derf, F.; Levillain, E.; Mazari, M.; Sallé, M.; Dubois, L.; Viel, P.; Bureau, C.; Palacin, S. *J. Am. Chem. Soc.* **2004**, *126*, 12194–12195. (c) Delogu, G.; Fabbri, D.; Dettori, M. A.; Sallé, M.; Le Derf, F.; Blesa, M.-J.; Allain, M. *J. Org. Chem.* **2006**, *71*, 9096–9103. (d) Lyskawa, J.; Le Derf, F.; Levillain, E.; Mazari, M.; Sallé, M. *Eur. J. Org. Chem.* **2006**, 2322–2328. (e) Blesa, M.-J.; Zhao, B.-T.; Allain, M.; Le Derf, F.; Sallé, M. *Chem. Eur. J.* **2006**, *12*, 1906–1914.

(9) The reduction potentials are referred to the first reduction waves of substituted quinones.

(10) (a) Ashton, P. R.; Balzani, V.; Becher, J.; Credi, A.; Fyfe, M. C. T.; Mattersteig, G.; Menzer, S.; Nielsen, M. B.; Raymo, F. M.; Stoddart, J. F.; Venturi, M.; Williams, D. J. *J. Am. Chem. Soc.* **1999**, *121*, 3951–3957. (b) Spanggaard, H.; Prehn, J.; Nielsen, M. B.; Levillain, E.; Allain, M.; Becher, J. *J. Am. Chem. Soc.* **2000**, *122*, 9486–9494. (c) Ribera, E.; Veciana, J.; Molins, E.; Mata, I.; Wurst, K.; Rovira, C. *Eur. J. Org. Chem.* **2000**, 2867–2875. (d) Khodorkovsky, V.; Shapiro, L.; Krief, P.; Shames, A.; Mabon, G.; Gorgues, A.; Giffard, M. *Chem. Commun.* **2001**, 2736–2737.

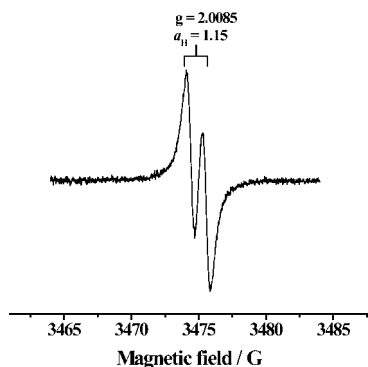


FIGURE 2. ESR spectrum of dyad **1** (1.0×10^{-4} M) in $\text{CH}_2\text{Cl}_2/\text{CH}_3\text{CN}$ (1:1, v/v) in the presence of 1.0 equiv of Pb^{2+} [$\text{Pb}(\text{ClO}_4)_2$] recorded at room temperature; the solution was degassed before measurement.

basis of the following considerations: (1) Intermolecular charge-transfer absorption bands were not detected for the mixture solutions of **6** (1.5×10^{-2} M) and **12/13/14** (2.5×10^{-2} M) (see Figure S15 of the Supporting Information). These results indicate that charge-transfer interactions between TTF and quinone units within dyads **1**, **2**, **3**, and **4** should be rather weak. (2) If these new absorption bands observed for dyads **1**, **2**, **3**, and **4** were due to the charge-transfer interactions, the corresponding charge-transfer absorption bands should be different since the electron accepting abilities of the quinone units within dyads **1**, **2**, **3**, and **4** are different. But, dyads **1**, **2**, **3**, and **4** exhibit the same new absorption bands at 450 and 845 nm upon addition of metal ions. The following ESR studies also indicate the formation of $\text{TTF}^{+\cdot}$ for these D–A dyads in the presence of metal ions. In short, these absorption spectral results clearly indicate the formation of $\text{TTF}^{+\cdot}$ in the presence of these metal ions (Pb^{2+} , Zn^{2+} , and Sc^{3+}), as a result of the electron transfer within these TTF–quinone dyads.¹¹

For each substituted TTF–quinone dyad, the absorption intensities at 450 and 845 nm (due to $\text{TTF}^{+\cdot}$) are rather weak in the presence of Zn^{2+} compared to those containing $\text{Pb}^{2+}/\text{Sc}^{3+}$. This result implies that $\text{Pb}^{2+}/\text{Sc}^{3+}$ can promote more efficiently the electron transfer between TTF and quinone units within these dyads, which is in agreement with the previous observation.⁶ Among these substituted TTF–quinone dyads, dyad **2** exhibits the strongest absorptions at 450 and 845 nm in the presence of metal ions under the same conditions. The absorption intensity at 845 nm decreases in the following order: **2** > **5** > **1** > **3** > **4**, as indicated in the inset of Figure 1 where the partial absorption spectra of dyads **1**, **2**, **3**, **4**, and **5** (5.0×10^{-5} M in a mixture of CH_2Cl_2 and CH_3CN (1:1, v/v)) containing 1.0 equiv of Pb^{2+} were displayed. A similar pattern of the difference in absorption intensity at 845 nm was observed in the presence of $\text{Sc}^{3+}/\text{Zn}^{2+}$ (see Figure S12 of the Supporting Information).

ESR signals were detected for dyads **1**, **2**, **3**, and **4** when metal ions were present. As an example, Figure 2 shows the ESR spectrum of dyad **1** in the presence of 1.0 equiv of Pb^{2+} . On the basis of previous reports,⁶ the doublet ESR signals were ascribed to the splitting of one H atom of the TTF unit in the radical cation of the TTF unit of dyad **1** ($g = 2.0085$, $a_{\text{H}} = 1.15$ G). The radical anion of quinone ($\text{Q}^{\cdot-}$) can be easily

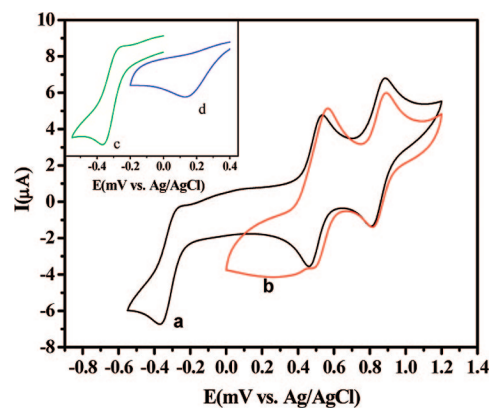


FIGURE 3. Cyclic voltammograms of dyad **12** (5.0×10^{-4} M) (a, black) before and (b, red) after addition of 2 equiv of Pb^{2+} in $\text{CH}_2\text{Cl}_2/\text{CH}_3\text{CN}$ (1:1, v/v) at a scan rate of 100 mV S^{-1} . The inset shows the cyclic voltammograms of compound **12** (5.0×10^{-4} M) before (c, green) and after addition of 2.0 equiv of $\text{Pb}(\text{ClO}_4)_2$ (d, blue) at a scan rate of 100 mV S^{-1} .

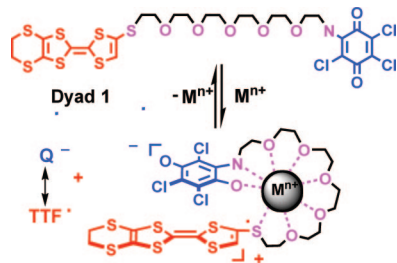
disproportionated into the corresponding Q^{2-} and neutral Q in the presence of metal ion at room temperature, which accounts for the absence of ESR signals related to the radical anion of the quinone ($\text{Q}^{\cdot-}$) unit of dyad **1**.^{6,12} Similar ESR spectra were observed for dyads **2**, **3**, and **4** after addition of Pb^{2+} (see Figures S16–S18 of the Supporting Information). These ESR spectral results also indicate that intramolecular electron transfer occurs between the TTF and quinone units within dyads **1**, **2**, **3**, and **4** in the presence of metal ions. For each substituted TTF–quinone dyad, the ESR signal intensity was higher in the presence of $\text{Pb}^{2+}/\text{Sc}^{3+}$ than that in the presence of Zn^{2+} under the same conditions. Among these substituted TTF–quinone dyads, dyad **2** exhibits the strongest ESR signal in the presence of metal ions under the same conditions. The ESR signal intensity of the solution of dyads **1**, **2**, **3**, **4**, and **5** decreases in the following order under the same conditions: **2** > **5** > **1** > **3** > **4**.

Both absorption and ESR spectral studies indicate that the metal ion-promoted electron transfer occurs within the substituted TTF–quinone dyads **1**, **2**, and **3**, even for dyad **4**, which features a rather weak electron acceptor unit. The metal ion-promoted electron transfer can be ascribed to the positive shift of reduction potentials of quinones in the presence of metal ions and the synergic coordination of oligoethylene glycol chain and the radical anion of quinone with metal ions. The cyclic voltammograms of dyads **1**, **2**, **3**, and **4** and reference quinones **12**, **13**, **14**, and **15** were measured in the presence of $\text{Pb}^{2+}/\text{Sc}^{3+}/\text{Zn}^{2+}$ (see Figures S20–S34 of the Supporting Information). By employing the Fukuzumi's method,^{12,13} the reduction potentials of reference compounds **12**, **13**, **14**, and **15** were estimated to be 0.22, 0.28, 0.19, and 0.06 V, respectively, in the presence of 4.0 equiv of Pb^{2+} . As an example, Figure 3 shows the cyclic voltammogram of dyad **1** containing 2.0 equiv of Pb^{2+} . The reduction wave around -0.36 V due to the redox reaction ($\text{Q}/\text{Q}^{\cdot-}$) disappeared after addition of Pb^{2+} , and the anodic current around 0.48 V increased. It is probable that the reduction potential of the quinone unit of dyad **1** was shifted from -0.36 to 0.48 V in the presence of Pb^{2+} .¹⁴ On the basis of these electrochemical data, it can be concluded that the electron

(11) The disproportionation reaction of $\text{Q}^{\cdot-}$ into the corresponding Q^{2-} and neutral Q unit may occur easily in the presence of metal ions at room temperature (see ref 10). This is in agreement with the fact that no ESR signals due to the $\text{Q}^{\cdot-}$ were detected for the solutions of dyad **1** after addition of metal ions at room temperature.

(12) Fukuzumi, S.; Nishizawa, N.; Tanaka, T. *J. Chem. Soc., Perkin Trans. II* **1985**, 371–378.

(13) Fukuzumi, S.; Hironaka, K.; Nishizawa, N.; Tanaka, T. *Bull. Chem. Soc. Jpn.* **1983**, 56, 2220–2227.

SCHEME 2. The Proposed Mechanism for the Metal Ion-Promoted Electron Transfer within Dyad 1


transfer between TTF and quinone units of dyads **1**, **2**, **3**, and **4** would become thermodynamically more feasible in the presence of these metal ions (Pb^{2+} , Sc^{3+} , and Zn^{2+}). The reduction potential of reference compound **13** is higher than those of **12**, **14**, and **15** in the presence of $\text{Pb}^{2+}/\text{Sc}^{3+}/\text{Zn}^{2+}$. Their differences in reduction potentials in the presence of metal ions may explain why dyad **2** showed the strongest absorption and ESR signals as mentioned above.

The electron transfer processes within dyads **1**, **2**, **3**, and **4** are still endothermic by just considering the redox potentials of the TTF ($E^{1/2}(\text{ox}_1) = 0.50\text{V}$, $E^{1/2}(\text{ox}_2) = 0.84\text{V}$ as discussed above) and quinone units in the presence of metal ion (Pb^{2+} , Sc^{3+} , Zn^{2+}). Particularly, the quinone unit of dyad **4** exhibited rather low reduction potential. Therefore, other mechanisms must also contribute to the observed electron transfer in the dyads, which could be the synergic coordination of oligoethylene glycol chain and the radical anion of the quinone unit with metal ion (see Scheme 2). This explains why electron transfer can be observed for dyad **4**, which contains a rather weak electron acceptor. The observation that $\text{Pb}^{2+}/\text{Sc}^{3+}$ can promote the electron transfer within TTF–quinone dyads efficiently may be understood this way: (1) Sc^{3+} shows a preference for oxygen coordination and (2) apart from the oxygen atoms of the oligoethylene glycol chains, the sulfur atoms of the TTF unit also may be involved in the coordination with metal ions, in particular for Pb^{2+} , which is a very poor oxyophile and prefers the much softer sulfur ligands.

In summary, four new substituted TTF–quinone dyads were synthesized and investigated in the presence of metal ions with a view to understanding the influences of the electron-accepting abilities of quinone units on the metal ion-promoted electron-transfer process. The results indicate that (1) the metal ion-

(14) Compared to compound **12**, the reduction potential of the quinone unit of dyad **1** was further shifted anodically. This is likely due to the synergic coordination of oligoethylene glycol chain and the radical anion of quinone with metal ions as shown in Scheme 2, which would further facilitate the electron transfer process within dyad **1**.

promoted electron transfer occurs to all new dyads including dyad **4**, which features a rather weak electron acceptor unit, and (2) the metal ion-promoted electron transfer within the dyads **1**, **2**, **3**, and **4** is influenced by the electron-accepting abilities of quinone units: dyad **2** with a strong electron acceptor shows strong absorption and ESR signals due to TTF^+ in the presence of metal ions, compared to dyad **4** with a weak electron acceptor under the same conditions. Moreover, the fact that metal ion-promoted electron transfer occurs to dyad **4** with a rather weak electron acceptor supports the assumption that the synergic coordination of oligoethylene glycol chain and the radical anion of the quinone unit with the metal ion may contribute to stabilizing the corresponding charge-separation state and thus facilitate the electron-transfer process.

Experimental Section

Synthesis of Dyad 1. A solution of **10** (0.5 g, 0.81 mmol) in THF (60 mL) was treated with PPh_3 (0.43 g, 1.62 mmol) and H_2O (0.2 mL, 11.1 mmol) at 25 °C under N_2 . The resulting reaction mixture was warmed at 45 °C for 10 h. The reaction mixture was diluted with water and extracted with CH_2Cl_2 . The organic phase was dried over MgSO_4 and concentrated in vacuo to give crude **11** as a yellow oil that was used directly without further purification.

The crude product of **11** was dissolved in dry THF and the solution was cooled to 0 °C. Tetrachloro-1,4-benzoquinone (0.37 g, 1.5 mmol) was added. After being stirred for 30 min at this temperature the reaction mixture was concentrated in vacuo. Column chromatography of the residue on silica gel with $\text{CH}_2\text{Cl}_2/\text{EtOAc}$ (6:1, v/v) as eluant afforded dyad **1** as a purple oil (0.20 g) in 31% yield: ^1H NMR (400 MHz, CDCl_3) δ 6.42 (1H, s), 4.00 (2H, m), 3.71 (2H, t, $J = 5.1\text{ Hz}$), 3.66–3.62 (18H, m), 3.29 (4H, s), 2.93 (2H, t, $J = 6.4\text{ Hz}$); ^{13}C NMR (100 MHz, CDCl_3) δ 174.3, 170.0, 143.6, 142.8, 135.9, 126.8, 123.1, 114.1, 106.9, 70.9, 70.8, 70.77, 70.74, 70.67, 69.8, 69.7, 44.9, 35.5, 30.4; HR-MS (MALDI-TOF) calcd for $\text{C}_{26}\text{H}_{30}\text{Cl}_3\text{NO}_7\text{S}_7$ 796.9133, found 796.9092. Due to overlapping signals, the total number of ^{13}C NMR signals deviates from the total carbon number within dyad **1**. This also holds true for dyads **2**, **3**, and **4**.

The synthesis and characterization of dyads **2**, **3**, and **4** are provided in the Supporting Information.

Supporting Information Available: Synthesis of dyads **2**, **3**, and **4** and compounds **12–15**, absorption and ESR spectra of dyads **1**, **2**, **3**, and **4** in the presence of metal ions, cyclic voltammograms of **1**, **2**, **3**, and **4**, and compounds **12–15**, and those in the presence of metal ions, ^1H NMR and ^{13}C NMR of dyads **1**, **2**, **3**, and **4** and compounds **7**, **8**, **10**, **12**, and **15**. This material is available free of charge via the Internet at <http://pubs.acs.org>.

JO800581T